Metallaheteroborane Chemistry. Part 5.[1] Synthesis of *closo*-[2,2-$(PR_3)_2$-1,2-$SePtB_{10}H_{10}$] (R_3 = Et_3, $Bu^n{}_3$, or Me_2Ph) and *arachno*-[9,9-$(PMe_2Ph)_2$-6,9-$SePtB_8H_{10}$] and their Characterisation by Nuclear Magnetic Resonance Techniques: The Crystal and Molecular Structures of *closo*-[2,2-$(PEt_3)_2$-1,2-$SePtB_{10}H_{10}$] and *arachno*-[9,9-$(PMe_2Ph)_2$-6,9-$SePtB_8H_{10}$]†

Faridoon, Orla Ni Dhubhghaill, and Trevor R. Spalding *
Chemistry Department, University College, Cork, Ireland
George Ferguson * and Branko Kaitner
Chemistry Department, University of Guelph, Guelph, Ontario, N1G 2W1, Canada
Xavier L. R. Fontaine and John D. Kennedy
School of Chemistry, University of Leeds, Leeds LS2 9JT

The *closo* compounds [2,2-$(PR_3)_2$-1,2-$SePtB_{10}H_{10}$], where R_3 = Et_3 (**1**) or $Bu^n{}_3$ (**2**), have been isolated in low-to-moderate yield from the reaction between *cis*-[$PtCl_2(PR_3)_2$] and *nido*-[7-$SeB_{10}H_{11}$]$^-$ in tetrahydrofuran. Both *closo*-[2,2-$(PMe_2Ph)_2$-1,2-$SePtB_{10}H_{10}$] (**3**) and *arachno*-[9,9-$(PMe_2Ph)_2$-6,9-$SePtB_8H_{10}$] (**4**) were isolated from the reaction with R_3 = Me_2Ph. N.m.r. spectroscopy confirms the general structures of the compounds, and variable-temperature ^1H-{^{31}P} experiments on (**3**) show the rotational metal-to-heteroborane bonding fluxionality to have $\Delta G^{\ddagger}_{328}$ *ca.* 58 kJ mol^{-1}. An *X*-ray diffraction study of compound (**1**) shows the orthorhombic crystals belong to the space group *Fdd2*, with *Z* = 16 and cell dimensions *a* = 55.052(6), *b* = 17.842(5), and *c* = 10.259(4) Å, *R* = 0.042 for 2 551 observed reflections. Cage interatomic distances involving Pt or Se are Pt–Se 2.676(2), Pt–B 2.23(2)—2.32(2), and Se–B 2.08(2)—2.20(2) Å. Crystals of (**4**) are orthorhombic, space group $P2_1nm$ with *a* = 6.935(1), *b* = 10.048(2), and *c* = 17.413(2) Å, *R* = 0.022 for 1 375 observed reflections. Interatomic distances include Pt–B 2.147(10)—2.230(7) and Se–B 2.062(15)—2.113(8) Å. Both the *X*-ray crystallographic and n.m.r. results for (**4**) indicate this compound belongs to the *arachno* class. As a model for (**4**), the bonding of the PtP_2 unit to the heteroborane SB_8H_{10} ligand has been analysed in a frontier-orbital approach.

In Part 1 of this series we reported that the reaction of $SeB_{11}H_{11}$ and [$Pt(PPh_3)_4$] afforded twelve-vertex *closo*-[2,2-$(PPh_3)_2$-1,2-$SePtB_{10}H_{10}$], the first platinaselenaborane.[2] We confirmed the *closo* nature of the cluster by n.m.r. spectroscopy and *X*-ray diffraction analysis. Prior to this, the initial work in the field of platinachalcogenaboranes had concerned the preparation of the twelve-vertex *closo* complex [$(PEt_3)_2PtSB_{10}H_{10}$],[3] the eleven-vertex *nido* complex [$(PEt_3)_2HPtB_9H_{10}$][3] and a series of compounds formulated at the time as the *closo* eleven-vertex species [$(L_2M)SB_9H_9$] (M = Pt or Pd, L = PPh_3).[4] The *closo*-$PtSB_{10}$ derivative was isolated in 29% yield from the reaction between [$PtCl_2(PEt_3)_2$] and *nido*-[$SB_{10}H_{10}$]$^{2-}$ in tetrahydrofuran (thf)–hexane solvent, the *nido*-$PtSB_9$ derivative from the *arachno*-[SB_9H_{12}]$^-$ anion and [$PtHCl(PEt_3)_2$], and the other compounds were formed in the reaction between *nido*-[SB_9H_9]$^{2-}$ and [$MCl_2(PPh_3)_2$]. Later studies by Rudolph and co-workers[5] established that the reaction of *closo*-SB_nH_n (*n* = 9 or 11) with platinum(0) complexes [$Pt(PR_3)_4$] in ethanol gave ten-vertex products of the general formula [9,9-$(PR_3)_2$-6,9-$SPtB_8H_{10}$] (PR_3 = PPh_3, PMe_2Ph, or PEt_3), and a B-ethoxy derivative, [8-OEt-9,9-$(PPh_3)_2$-6,9-$SPtB_8H_9$], was also isolated. The ten-vertex complex [9,9-$(PPh_3)_2$-6,9-$SPtB_8H_{10}$] has also been obtained from the reaction between [$Pt(PPh_3)_4$] and *nido*-4-SB_8H_{12} in benzene.[6] Two of the ten-vertex $SPtB_8$ compounds have been characterised by single-crystal *X*-ray analyses which showed boat-like *arachno* structures (I) with Pt and S not bonded.[5,6] As a result of the close similarity between the ^{11}B n.m.r. spectra of $SPtB_8$ species[5] and those[4] of the compounds formulated as eleven-vertex *closo* $SPtB_9$ derivatives,[6] a reassessment of the constitution of the latter compounds as $SPtB_8$ species has been suggested.[5]

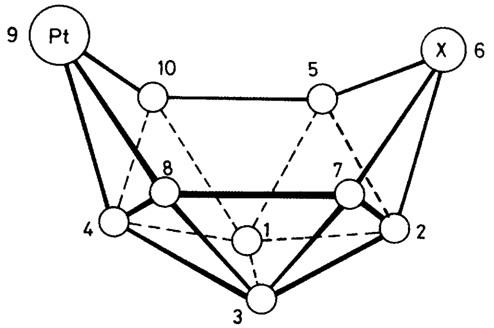

(I)

In this paper we report the synthesis and characterisation of three further twelve-vertex *closo* platinaselenaboranes of the type [2,2-$(PR_3)_2$-1,2-$SePtB_{10}H_{10}$], now with R_3 = Et_3 (**1**),

---

† 2,2-Bis(triethylphosphine)-1-selena-2-platina-*closo*-dodecaborane and 9,9-bis(dimethylphenylphosphine)-6-selena-9-platina-*arachno*-decaborane.

Supplementary data available: see Instructions for Authors, *J. Chem. Soc., Dalton Trans.*, 1989, Issue 1, pp. xvii—xx.

Non-S.I. unit employed: eV ≈ 1.60 × 10^{-19} J.

Table 1. Measured n.m.r. parameters for *closo*-$[2,2\text{-}(PR_3)_2\text{-}1,2\text{-}SePtB_{10}H_{10}]$ (**1**)—(**3**)^{a} and the (R = Ph) analogue^{b} in CD_2Cl_2 solution, δ/p.p.m. and *J*/Hz

Assignment^{c} (intensity)	$[2,2\text{-}(PMe_2Ph)_3\text{-}1,2\text{-}SePtB_{10}H_{10}]$ (**3**), 294 K^{a}				(**1**) R = Et	(**2**) R = Bu^{n}	R = Ph	
	$\delta(^{11}B)^{d,e}$	$\delta(^{1}H)^{f}$	$^{1}J(^{11}B\text{–}^{1}H)^{g}$	$^{n}J(^{195}Pt\text{–}^{1}H)^{h}$	$\delta(^{11}B)$	$\delta(^{11}B)$	$\delta(^{11}B)^{e}$	$\delta(^{1}H)^{i}$
(12) (1BH)	+17.5	+4.25	138	+58.7 (^{3}J)	+18.5	+18.3	+18.5	+4.08
(7,11) (2BH)	+5.2^{j}	+3.39	*ca.* 145^{g}	−21.6 (^{2}J)	+5.9	+5.8	*ca.* +6.7^{k} } ^{l}	{ +3.47
(9) (1BH)	+3.85	+5.48	*ca.* 165^{g}	*ca.* +25 (^{4}J)	+4.0	+3.7	*ca.* +6.7 }	{ +5.27
(3,6) (2BH)	−5.5^{m}	+1.31	134	*ca.* 0 (^{2}J)	−5.7	+5.5	−2.1	+1.37
(4,5) (2BH)	−13.1	+2.58	157	*ca.* +10 (^{2}J)	−12.1	−12.2	−12.2	+2.33
(8,10) (2BH)	−22.2	+1.58	142	*ca.* +30 (^{3}J)	−22.1	−22.3	−20.9	+1.20
(2)	[Pt]^{n,o}	+1.83^{o,p,q} +1.55^{o,p,q}		(+) 25.5 (^{3}J)^{p} (+) 30.7 (^{3}J)^{p}	[Pt]	[Pt]	[Pt]	

^{a} This work. ^{b} Data from ref. 2; assignments this work. ^{c} Assignments by relative intensities, incidence of ^{195}Pt satellites, and by $[^{1}H\text{–}^{1}H]$- and $[^{11}B\text{–}^{11}B]$-COSY cross-peaks, all these being very similar to those for the direct tellurium analogue described in ref. 7 (see Figure 2). ^{d} ±0.5 p.p.m. ^{e} Relative to $BF_3(OEt_2)$, zero. ^{f} $\delta(^{1}H)$ Assigned to directly bound B atoms by $^{1}H\text{-}\{^{11}B(\text{selective})\}$ experiments. ^{g} ±8 Hz; measured from resolution-enhanced ^{11}B spectra; peak overlap precludes accurate measurements for BH(7,11) and BH(9). ^{h} Signs measured relative to $^{1}J[^{195}Pt\text{–}^{11}B(7,11)]$ (footnote *j*) taken as positive, and established by $^{1}H\text{-}\{^{11}B(\text{selective})\}$ experiments (*cf.* ref. 19) or by the 'tilted lozenge' effect in $[^{1}H\text{–}^{1}H]$-COSY spectra (*cf.* ref. 7 and also Figure 4 in the present work for a similar effect in the $[^{11}B\text{–}^{11}B]$-COSY spectrum). ^{i} $\delta(^{1}H)$ not assigned and not related to $\delta(^{11}B)$ in ref. 2; here assigned by analogy with compound (**1**). ^{j} $^{1}J(^{195}Pt\text{–}^{11}B)$ 235 Hz. ^{k} $^{1}J(^{195}Pt\text{–}^{11}B)$ *ca.* 225 Hz. ^{l} Accidentally coincident resonances. ^{m} No ^{195}Pt satellites resolved, implying $^{1}J(^{195}Pt\text{–}^{11}B) <$ *ca.* 80 Hz. ^{n} $\Xi(^{195}Pt)$ 21.386 920 MHz. ^{o} $^{1}J(^{195}Pt\text{–}^{31}P)$ 3 099 ± 7 Hz; $\delta(^{31}P)$ −12.3 p.p.m. ($w_{\frac{1}{2}}$ 21 Hz). ^{p} P-methyl resonances measured at 243 K [at 290 K (400 MHz) coalescence occurs to give one resonance position]. ^{q} $N(^{31}P\text{–}^{1}H)$ 10 Hz; $\delta(^{1}H)$(Ph) +7.6 to +7.3 p.p.m.

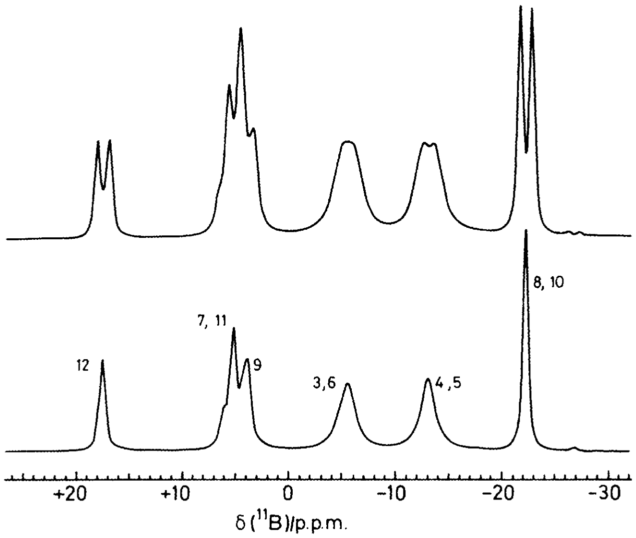

Figure 1. 128-MHz ^{11}B n.m.r. spectra for *closo*-$[2,2\text{-}(PMe_2Ph)_2\text{-}1,2\text{-}SePtB_{10}H_{10}]$ (**3**). The top trace is the straightforward spectrum, and the bottom trace is the same spectrum recorded under conditions of $\{^{1}H$ (broad-band noise)$\}$ decoupling. Note the presence of ^{195}Pt satellites for the $^{11}B(7,11)$ resonance

Bu^{n}_3 (**2**), and Me_2Ph (**3**), together with the isolation and characterisation of $[9,9\text{-}(PMe_2Ph)_2\text{-}6,9\text{-}SePtB_8H_{10}]$ (**4**), which is the first selenium-containing *arachno*-$PtXB_8$ complex. All these compounds were obtained by a different route to that previously described by us.[2]

Results and Discussion

Preparation of Compounds (**1**)—(**4**).—The reaction between $[NR_4][7\text{-}nido\text{-}SeB_{10}H_{11}]$ ($NR_4 = NEt_3H$ or NEt_4) and the platinum(II) complexes $[PtCl_2(PR_3)_2]$ ($R_3 = Et_3$, Bu^{n}_3, or Me_2Ph) in 1:1 molar ratio in refluxing thf solution gave in each case between five and seven products most of which were in yields which were too low to be viable for characterisation. Separation and purification, by preparative t.l.c., from the reaction where R = Et or Bu^{n}, yielded in each case one major product which was characterised as *closo*-$[2,2\text{-}(PR_3)_2\text{-}1,2\text{-}SePtB_{10}H_{10}]$ (see below). In the case of $R_3 = Me_2Ph$, two products were isolated which, after recrystallisation from CH_2Cl_2, were shown to be *closo*-$[2,2\text{-}(PMe_2Ph)_2\text{-}1,2\text{-}SePtB_{10}H_{10}]$ (**3**) and *arachno*-$[9,9\text{-}(PMe_2Ph)_2\text{-}6,9\text{-}SePtB_8H_{10}]$ (**4**).

The i.r. spectra of compounds (**1**)—(**4**) showed strong B–H stretching bands: (**1**) 2 560s, 2 540w, 2 520vs, and 2 490w; (**2**) 2 560s and 2 520vs; (**3**) 2 550s, 2 505vs, and 2 485w; and (**4**) 2 550s, 2 530s, 2 515w, 2 495s, and 2 455s cm^{-1}. The i.r. spectra of (**1**)—(**3**) are similar in general to those of the corresponding tellurium analogues.[7]

N.M.R. Investigation of the closo *Twelve-vertex Compounds* (**1**)—(**3**).—Compounds (**1**)—(**3**) were readily characterised by their detailed n.m.r. behaviour (Table 1 and Figures 1 and 2). All show relative intensity patterns of 1:2:1:2:2:2 in the ^{11}B n.m.r. spectra. Their overall ^{11}B and ^{1}H shielding, coupling, and correlation-spectroscopy (COSY) correlation patterns are directly analogous to those of the previously reported tellurium compounds.[7] They are also consistent with the data previously obtained for the *closo*-$[2,2\text{-}(PPh_3)_2\text{-}1,2\text{-}SePtB_{10}H_{10}]$ complex (**5**),[2] which are also shown in Table 1 for comparison, with the overall similarities now permitting the previously reported spectrum of (**5**) to be assigned.

In the ^{11}B and ^{1}H n.m.r. spectra the most marked difference between the selenium and tellurium species are the *ca.* 1.5 p.p.m. changes in $\delta(^{1}H)$ for the BH(12) positions antipodal to the chalcogen, the heavier chalcogen inducing a lower shielding for these protons. A similar proton deshielding effect is observed for the BH(9) position antipodal to the heavier metal in the species *closo*-$[2,2\text{-}(PPh_3)_2\text{-}2\text{-}H\text{-}1,2\text{-}TeMB_{10}H_{10}]$ as M is changed from rhodium to iridium,[1] and may have use as a general diagnostic for heavier atoms in this type of *closo* system. Other changes observed for the selenium *versus* the tellurium compound are increases in $^{1}J(^{195}Pt\text{–}^{31}P)$ and $^{3}J(^{195}Pt\text{–}P\text{–}C\text{–}^{1}H)$, both expected with an increase in effective electronegativity of the ligand opposite the phosphines, and there was also a shift in $\delta(^{195}Pt)$ of 268 p.p.m. to higher frequency (lower shielding) compared to the tellurium species.

For the $Pt(PMe_2Ph)_2$ compound (**3**), the activation energy $\Delta G^{\ddagger}$, for the fluxional process in which the $Pt(PR_3)_2$ unit appears

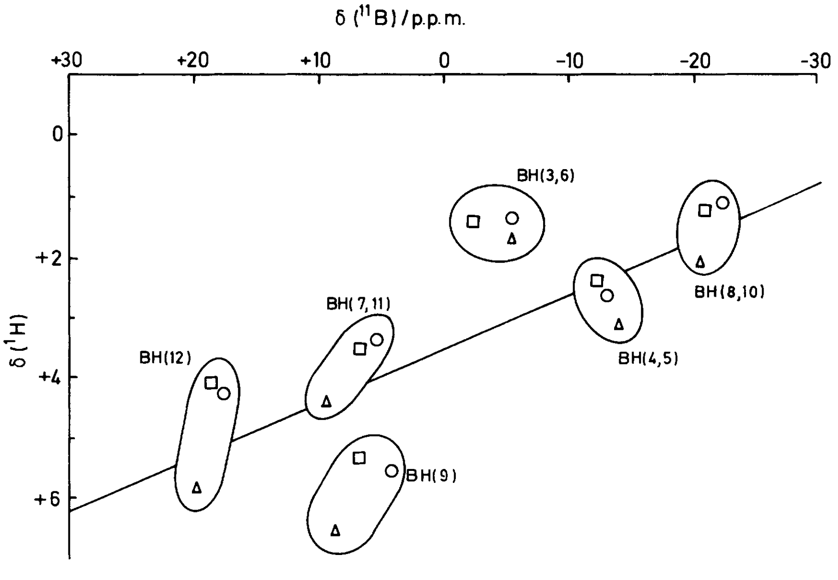

Figure 2. Plot of $\delta(^{11}B)$ *versus* $\delta(^{1}H)$ of directly bound B–H(*exo*) units for $[2,2\text{-}(PMe_2Ph)_2\text{-}1,2\text{-}SePtB_{10}H_{10}]$ (3) (○), its $(PPh_3)_2$ analogue (data from ref. 2) (□), and its tellurium analogue $[2,2\text{-}(PMe_2Ph)_2\text{-}1,2\text{-}TePtB_{10}H_{10}]$ [data from ref. 6 (△)], all measured in CD_2Cl_2 solution. The line drawn has slope $\delta(^{11}B):\delta(^{1}H)$ of 11:1, intercept $\delta(^{1}H)$ +3.5

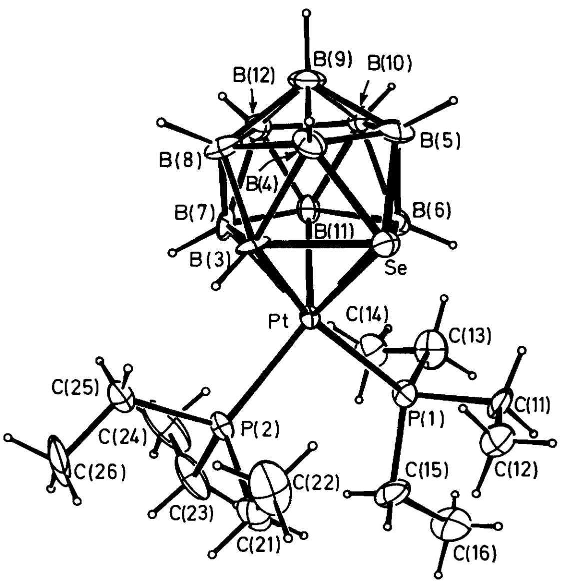

Figure 3. ORTEP plot of *closo*-$[2,2\text{-}(PEt_3)_2\text{-}1,2\text{-}SePtB_{10}H_{10}]$ (1) with the boron cage numbering scheme; ellipsoids are at the 20% level

to rotate above the SeB_4 face,[7] was measured by n.m.r. peak coalescence in the $^{1}H\text{-}\{^{31}P\}$ spectra to be *ca.* 58 kJ mol^{-1}. This is significantly less, by some 4 kJ mol^{-1}, than that reported for the tellurium species in ref. 7. Note that in Figure 6(*b*) of ref. 7 the spectrum is a $^{1}H\text{-}\{^{31}P$(broad-band noise)$\}$ one.

Molecular Structure of the closo *Compound* (1).—Crystallisation of (1) from dichloromethane–hexane solution afforded orange crystals suitable for single-crystal *X*-ray diffraction analysis. The analysis establishes the *closo* geometry of the compound (Figure 3), in accord with the n.m.r. studies. The overall cage structure is the same as that observed in *closo*-$[2,2\text{-}(PPh_3)_2\text{-}1,2\text{-}SePtB_{10}H_{10}]$ (5)[2] and *closo*-$[2,2\text{-}(PEt_3)_2\text{-}1,2\text{-}TePtB_{10}H_{10}]$ (6),[7] *i.e.* a distorted dodecahedron in which the $Pt(PR_3)_2$ unit is bonded to an XB_4 ring. A list of selected interatomic distances and angles is given in Table 2. The conformation of the PtP_2 unit over the SeB_4 face is essentially the same as in each of the previously characterised Pt–Se[2] and Pt–Te[7] compounds and may be rationalised in terms of highest occupied molecular orbital–lowest unoccupied molecular orbital (h.o.m.o.–l.u.m.o.) interactions between the $Pt(PR_3)_2$ and $XB_{10}H_{10}$ units (X = S or Se and Te respectively).[2,7]

Comparison of the interatomic distances between platinum and the atoms P(1), P(2), Se, B(3), B(7), B(11), and B(6) in (1) with the corresponding distances in compound (5)[2] reveals that the icosahedral $PtSeB_{10}$-cage dimensions are virtually identical although the Pt–P distances in (1) are slightly smaller than those in (5). Thus the change in ligand on platinum from PPh_3 to PEt_3 has not affected the cage bonding significantly.

In compound (1) the bonding distances between the selenium or platinum atom and the boron atoms B(3) and B(6), *i.e.* the boron atoms which are attached to both selenium and platinum atoms, are longer than the other selenium–boron and platinum–boron distances. Similar variations have been previously found with other metallaheteroboranes[1,2,7] and reflect steric effects of the adjacent heteroatoms; both the shortest and longest platinum–boron distances, 2.23(2) and 2.32(2) Å respectively, are within the 'normal range.' The smaller value is 0.11 Å longer than the shortest platinum–boron distances reported, 2.12(1) Å in $[(PMe_2Ph)_2Pt\text{-}\sigma,\eta^2\text{-}anti\text{-}B_{18}H_{20}]$.[8] The selenium–boron distances vary in the range 2.08(2) to 2.20(2) Å. The corresponding range for the analogous compound (5) is 2.098(9)—2.210(6) Å.

The platinum–phosphorus bond lengths in (1) are essentially equal [2.311(4) and 2.316(4) Å] and the same as in $[2,7\text{-}Me_2\text{-}9,9\text{-}(PEt_3)_2\text{-}9,2,7\text{-}PtC_2B_7H_7]$.[9] In the majority of compounds containing the PtP_2 unit the platinum–phosphorus bonds are not equal.[1,2,7,10,11]

The interboron distances in compound (1) range from 1.71(3) to 1.96(3) Å. Of these, the longest are observed for the boron atoms that are attached to both the selenium and platinum atoms, *i.e.* for B(3) and B(6). The average of the six boron–boron interactions involving either B(3) or B(6) is 1.86 Å while the average of the fifteen interactions not involving B(3) or B(6) is

Table 2. Molecular dimensions of $[2,2\text{-}(PEt_3)_2\text{-}1,2\text{-}SePtB_{10}H_{10}]$ (**1**); distances in Å, angles in °

Pt–Se	2.676(2)	P(1)–C(11)	1.84(2)	C(25)–C(26)	1.46(3)	B(6)–B(11)	1.83(2)
Pt–P(1)	2.316(4)	P(1)–C(13)	1.84(2)	B(3)–B(4)	1.93(3)	B(7)–B(8)	1.79(3)
Pt–P(2)	2.311(4)	P(1)–C(15)	1.82(2)	B(3)–B(7)	1.87(3)	B(7)–B(11)	1.78(3)
Pt–B(3)	2.32(2)	P(2)–C(21)	1.84(2)	B(3)–B(8)	1.75(3)	B(7)–B(12)	1.77(3)
Pt–B(6)	2.28(2)	P(2)–C(23)	1.83(2)	B(4)–B(5)	1.81(3)	B(8)–B(9)	1.78(3)
Pt–B(7)	2.23(2)	P(2)–C(25)	1.84(2)	B(4)–B(8)	1.74(3)	B(8)–B(12)	1.76(3)
Pt–B(11)	2.26(2)	C(11)–C(12)	1.53(3)	B(4)–B(9)	1.72(3)	B(9)–B(10)	1.77(3)
Se–B(3)	2.18(2)	C(13)–C(14)	1.46(4)	B(5)–B(6)	1.96(3)	B(9)–B(12)	1.74(3)
Se–B(4)	2.09(2)	C(15)–C(16)	1.48(3)	B(5)–B(9)	1.71(3)	B(10)–B(11)	1.81(3)
Se–B(5)	2.08(2)	C(21)–C(22)	1.53(3)	B(5)–B(10)	1.76(3)	B(10)–B(12)	1.75(3)
Se–B(6)	2.20(2)	C(23)–C(24)	1.51(4)	B(6)–B(10)	1.82(3)	B(11)–B(12)	1.76(3)

Angles around Pt, Se, P(1), P(2), C(11), (C13), C(15), C(21), C(23), C(25)

Se–Pt–P(1)	105.9(1)	P(2)–Pt–B(7)	98.3(5)	B(3)–Se–B(4)	53.8(7)	Pt–P(2)–C(21)	117.4(6)
Se–Pt–P(2)	119.7(1)	P(2)–Pt–B(11)	137.1(5)	B(3)–Se–B(5)	90.8(8)	Pt–P(2)–C(23)	115.6(7)
Se–Pt–B(3)	51.1(5)	B(3)–Pt–B(6)	82.6(6)	B(3)–Se–B(6)	87.9(6)	Pt–P(2)–C(25)	115.3(7)
Se–Pt–B(6)	51.9(4)	B(3)–Pt–B(7)	48.5(6)	B(4)–Se–B(5)	51.6(8)	C(21)–P(2)–C(23)	103(1)
Se–Pt–B(7)	88.1(4)	B(3)–Pt–B(11)	81.8(6)	B(4)–Se–B(6)	91.4(7)	C(21)–P(2)–C(25)	102.8(9)
Se–Pt–B(11)	87.8(5)	B(6)–Pt–B(7)	81.6(6)	B(5)–Se–B(6)	54.5(8)	C(23)–P(2)–C(25)	100.5(9)
P(1)–Pt–P(2)	98.5(2)	B(6)–Pt–B(11)	47.5(6)	Pt–P(1)–C(11)	112.6(5)	P(1)–C(11)–C(12)	112(1)
P(1)–Pt–B(3)	156.4(5)	B(7)–Pt–B(11)	46.9(7)	Pt–P(1)–C(13)	112.2(7)	P(1)–C(13)–C(14)	114(1)
P(1)–Pt–B(6)	85.5(5)	Pt–Se–B(3)	55.9(5)	Pt–P(1)–C(15)	122.0(6)	P(1)–C(15)–C(16)	117(2)
P(1)–Pt–B(7)	148.7(5)	Pt–Se–B(4)	100.9(6)	C(11)–P(1)–C(13)	103.1(7)	P(2)–C(21)–C(22)	113(2)
P(1)–Pt–B(11)	104.8(5)	Pt–Se–B(5)	100.6(6)	C(11)–P(1)–C(15)	102.6(9)	P(2)–C(23)–C(24)	113(2)
P(2)–Pt–B(3)	91.0(4)	Pt–Se–B(6)	54.9(5)	C(13)–P(1)–C(15)	102.0(9)	P(2)–C(25)–C(26)	118(2)
P(2)–Pt–B(6)	171.6(5)						

Selected interatomic angles around B(3)—B(7), B(9) (opposite Pt), B(11), and B(12) (opposite Se)

Pt–B(3)–Se	73.0(5)	B(3)–B(7)–B(11)	110(1)	B(4)–B(5)–B(9)	58(1)	B(6)–B(11)–B(7)	109(1)
Pt–B(3)–B(7)	63.3(8)	B(4)–B(9)–B(5)	64(1)	Pt–B(6)–Se	73.3(6)	B(7)–B(12)–B(8)	61(1)
Se–B(3)–B(4)	60.6(8)	B(4)–B(9)–B(8)	60(1)	Pt–B(6)–B(11)	65.5(8)	B(7)–B(12)–B(11)	61(1)
Se–B(3)–B(7)	115.5(9)	B(5)–B(9)–B(10)	61(1)	Se–B(6)–B(11)	117(1)	B(8)–B(12)–B(9)	61(1)
Se–B(4)–B(3)	65.5(9)	B(8)–B(9)–B(12)	60(1)	Pt–B(7)–B(3)	68.3(8)	B(9)–B(12)–B(10)	61(1)
Se–B(4)–B(5)	64.0(9)	B(10)–B(9)–B(12)	60(1)	Pt–B(7)–B(8)	119(1)	B(10)–B(12)–B(11)	62(1)
B(5)–B(4)–B(9)	58(1)	Pt–B(11)–B(6)	67.1(8)	Pt–B(7)–B(11)	67.5(9)		
Se–B(5)–B(4)	64(1)	Pt–B(11)–B(7)	65.7(9)				

1.76 Å. The same trend was also noted in compound (**5**), (**6**), and $[2,2\text{-}(PPh_3)_2\text{-}2\text{-}H\text{-}1,2\text{-}TeRhB_{10}H_{10}]$.[1]

N.M.R. Investigation of the arachno *Ten-vertex Compound* (**4**).—The species *arachno*-$[9,9\text{-}(PMe_2Ph)_2\text{-}6,9\text{-}SePtB_8H_{10}]$ (**4**) was characterised as such initially by n.m.r. spectroscopy. The measured n.m.r. parameters are in Table 3. The ^{11}B n.m.r. spectrum, Figure 4, consists of five peaks, intensity ratio 1:1:2:2:2, consistent with the molecular symmetry expected from the formulation. These resonances were readily assigned on the basis of (*a*) relative intensities, (*b*) the presence of coupling $^1J(^{195}Pt–^{11}B)$ to $^{11}B(4)$ and $^{11}B(8,10)$, and (*c*) the observed two-dimensional $[^{11}B–^{11}B]$-COSY cross-peaks, Figure 4. These last were observed for all nearest neighbours except for $^{11}B(2)–^{11}B(5,7)$ [which flank the Se atom (compare refs. 1, 2, 7, and 12)] and for the hydrogen-bridged B(5,7)–B(8,10) pairs. An interesting observation is the absence of low frequency/high frequency and high frequency/low frequency cross-correlations among the ^{195}Pt satellite lines of the $^{11}B(4)$ and $^{11}B(8,10)$ resonances, showing that the two couplings $^1J(^{195}Pt–^{11}B)$ are of the same sign, presumably positive [compare couplings $^1J(^{205}Tl–^{11}B)$ in ref. 13].

Selective $^1H\text{-}\{^{11}B\}$ experiments related the ^1H resonances to their directly bound boron positions, and also revealed that $^1H(5,10;7,8)$ (bridge) was more strongly coupled to $^{11}B(8,10)$, adjacent to the electropositive platinum centre, than to $^{11}B(5,7)$ adjacent to the more electronegative selenium (compare weaker $^{11}B–^{11}B$ couplings adjacent to the Se atom as mentioned above and in refs. 1 and 7, and compare with m.o. bonding considerations as discussed below). Two-dimensional $[^1H–^1H]$-COSY correlations were observed for all $^2J(^1H–^1H)$ and $^3J(^1H–^1H)$ borane cluster coupling pairs, confirming the positional assignments; interestingly there also appeared to be a weak $^4J(^1H–^1H)$ coupling between $^1H(4)$ and $^1H(5,7)$, although this was uncertain under the experimental conditions. Most of the cluster ^1H resonances exhibited satellite features arising from coupling to ^{195}Pt. Selective $^1H\text{-}\{^{11}B\}$ experiments, in which the ^{195}Pt satellites of the $^{11}B(4)$ and $^{11}B(8,10)$ resonances were irradiated, showed that the signs of $^2J(^{195}Pt–^1H)$ to $^1H(4)$, $^1H(8,10)$, and $^1H(5,10;7,8)$ (bridge) were all opposite to the corresponding $^1J(^{195}Pt–^{11}B)$ couplings, and therefore probably negative. In addition, the absence or presence of high-frequency/high-frequency or high-frequency/low-frequency cross-correlations among the ^{195}Pt satellites in the $[^1H–^1H]$-COSY spectrum,[7] when observed, confirmed these relative signs and also indicated that the couplings $^3J(^{195}Pt–^1H)$ to $^1H(1,3)$ [and probably also the antipodal coupling $^3J(^{195}Pt–^1H)$ to $^1H(2)$] were both positive in sign. There is a general parallel between the nuclear shielding of the ^1H *exo*-hydrogen atoms and their directly bound boron atoms, the slope of the correlation $\delta(^{11}B):\delta(^1H)$ of *ca.* 15:1 being more in line with other *nido* and *arachno* platinaborane species[14,15] than with *closo* species like compound (**3**) which have an approximate 11:1 correlation.[1,7]

The ^{195}Pt, ^{31}P, and ^1H n.m.r. parameters measured for the $Pt(PMe_2Ph)_2$ unit of compound (**4**) were similar to those previously reported[16] for the *arachno* nine- and ten-vertex species $[9,9\text{-}(PMe_2Ph)_2\text{-}9\text{-}PtB_8H_{12}]$ and [6,6,9,9-

Table 3. Measured n.m.r. parameters for *arachno*-[9,9-$(PMe_2Ph)_2$-6,9-$SePtB_8H_{10}$] (**4**) in CD_2Cl_2 solution at 294 K, δ/p.p.m. and *J*/Hz

Assignment[a]/ (Intensity)[b]	$\delta(^{11}B)$[c]	Observed $[^{11}B-^{11}B]$-COSY correlations[d,e]	$T_1(^{11}B)$/ms approx.	$^1J(^{11}B-^1H)$[f]	$\delta(^1H)$[c,g]	$^nJ(^{195}Pt-^1H)$[h]	Observed $[^1H-^1H]$-COSY correlations[e,i]
(4) (1BH)	+37.1[j]	(8,10)s (1,3)s [(9)s][k]	6	138	+5.21	−20.0 (^2J)[l]	(5,7)w_4 (8,10)m (1,3)s (μ)s[m]
(2) (1BH)	+6.2	(1,3)w	≤*ca.* 2[n]	169	+4.18	+36.0 (^4J)[o]	(5,7)w (1,3)s[m]
(5,7) (2BH)	−4.5	(1,3)s	≤*ca.* 2[n]	156	+3.10	*p*	(8,10)w (1,3)m (μ)s_2
(8,10) (2BH)	−17.5[q]	(4)s (1,3)m [(9)s][k]	4	134	+1.59	−24.0 (^2J)[l]	[r](4)m (5,7)w (μ)s_2
(1,3) (2BH)	−26.8	(4)s (2)w (5,7)s (8,10)m	10	143	+1.77	+62.0[n]	[r](4)s (2)s[m] (5,7)m (μ)s[m]
(9)	[Pt][s]	[(4)s (8,10)s][k]			+1.67[t] +1.72[t]	(+)27.4 (^3J)[t] (+)27.6 (^3J)[t]	
μ(7,8) and (5,10) (2H)				*u*	−1.51	−38.5[l,v]	(4)s[m] (5,7)s_2 (8,10)s_2[m] (1.3)s

[a] Assignments by relative intensities, incidence of couplings $^1J(^{195}Pt-^{11}B)$, and by $[^{11}B-^{11}B]$- and $[^1H-^1H]$-COSY cross-peaks. [b] Relative intensities in parentheses. [c] ±0.5 p.p.m. to low field of $BF_3(OEt_2)$. [d] Measured with $\{^1H$(broad-band noise)$\}$ decoupling. [e] s = Strong, w = weak, m = intermediate. [f] ±8 Hz, measured from the ^{11}B spectrum with resolution enhancement. [g] ±0.05 p.p.m.; $\delta(^1H)$ related to directly bound B atoms in $^1H-\{^{11}B$(selective)$\}$ experiments. [h] Signs measured relative to $^1J(^{195}Pt-^{11}B)$ taken as positive (see footnotes *l*, *m*, and *o*). [i] Measured with $\{^{11}H$(broad-band noise)$\}$ decoupling; note selective correlations among ^{195}Pt satellites between different resonance positions (see footnotes *l*, *m*, and *o*; also ref. 7; subscripts refer to *n* in ^nJ where $n \neq 3$. [j] $^1J(^{195}Pt-^{11}B)$ 285 Hz; see caption to Figure 4. [k] Refers to $^{195}Pt-^{11}B$ coupling; see footnotes *j* and *q*. [l] Relative sign by $^1H-\{^{11}B$(selective)$\}$ spectroscopy. [m] See footnote *o*. [n] Relaxation rate of $^{11}B(2)$ marginally faster than that of $^{11}B(5,7)$. [o] Relative sign by $[^1H-^1H]$-COSY spectroscopy among the ^{195}Pt satellites in the $^1H-\{^{11}B$(broad-band noise)$\}$ spectrum; relevant cross-peaks designated by superscript *m*. [p] Any $^3J(^{195}Pt-^1H)$ too small to be resolved. [q] $^1J(^{195}Pt-^{11}B)$ 250 Hz; see caption to Figure 4. [r] $\delta[^1H(1,3)]$ and $\delta[^1H(8,10)]$ too close for any mutual $[^1H-^1H]$-COSY correlation to be observed. [s] $\Xi(^{195}Pt)$ 21.380 630 MHz, $^1J(^{195}Pt-^{31}P)$ 2 731 ± 7 Hz. [t] P-methyl resonances (intensities 6H; 6H), $N(^{31}P-^1H)$ 9.2 Hz, in each case; $\delta(^1H)$(Ph) +7.4 to +7.2 p.p.m.; $\delta(^{31}P)$ −6.0 p.p.m. ($w_{\frac{1}{2}}$ 77 Hz). [u] Not measured. [v] Selectively sharpened much more by $\nu[^{11}B(8,10)]$ than by $\nu[^{11}B(5,7)]$ in $^1H-\{^{11}B$(selective)$\}$ experiments.

$(PMe_2Ph)_4$-6,9-$Pt_2B_8H_{10}$] which have analogous metal-to-borane bonding modes (see below). Unlike the *closo* compound (**3**) discussed above, there was no evidence for fluxionality in the metal-to-borane bonding in (**4**).

According to the n.m.r. results, therefore, (**4**) can be regarded in simple terms as an analogue of *arachno*-$[B_{10}H_{14}]^{2-}$ (or of *arachno*-$B_{10}H_{12}L_2$) in which $[BH_2]^-$ moieties at the 6 and 9 positions have been replaced by a selenium atom which contributes four electrons to the cluster bonding (see below) and a 16-electron square-planar platinum centre.[16–18] The ^{11}B n.m.r. shielding pattern with $^{11}B(2)$ and $^{11}B(4)$ at extreme low field and $^{11}B(1,3)$ at extreme high field is in accord with other *arachno*-decaboranes,[19] and is the converse of that observed in *nido*-decarboranyl systems [which have $^{11}B(2,4)$ at extreme high field and $^{11}B(1,3)$ at low field].[20]

The ten-atom platinaheteroborane (**4**) described in this work can therefore be regarded as one of a series of *arachno* compounds with the general formula $[L_2Pt(XB_8H_{10})]$, where L = PMe_2Ph and X = $Pt(PMe_2Ph)_2$ (**7**),[16] L = PPh_3 and X = NH (**8**),[21] CH_2 (**9**),[6] or S (**10**).[5,6] The ethoxy-substituted species $[(PPh_3)_2PtSB_8H_9(OEt)]$ (**11**),[5] and the PtX_2B_7 analogue, [9,9-$(PPh_3)_2$-5,6,9-$C_2PtB_7H_7$] (**12**),[22] may also be added for comparison. Interestingly, half of these compounds, *i.e.* (**9**)—(**11**), were originally classified as *nido* while the others, (**7**), (**8**), and (**12**) were classified as *arachno*. The *nido* categorisation of (**9**)—(**11**) was based mainly on the assumption that the PtP_2 unit supplies two electrons to cluster bonding [as may be assumed to occur in (**1**)—(**3**) above]. The *arachno* description of (**7**), (**8**), and (**12**) was based on the geometrical analogy of these compounds in the B–H–B bridging region with *arachno*-$[B_{10}H_{14}]^{2-}$,[23] and on the similarities in the n.m.r. shielding patterns. Comparison of known *nido*-$B_{10}H_{14}$[24] and *arachno*-$[B_{10}H_{14}]^{2-}$[23] species reveals that the main geometrical difference between the two cluster types lies in the position and number of the bridging hydrogens and the difference in the interboron distances in the B(5) to B(10) open face. In *arachno*-$[B_{10}H_{14}]^{2-}$ the H-bridged B(5)–B(10) and B(7)–B(8) distances are especially short at 1.882(12) and 1.892(12) Å respectively compared to the corresponding 'long' unbridged distance of 1.987(3) Å in *nido*-$B_{10}H_{14}$.[24]

Molecular Structure of the arachno-*Platinaselenaborane* (**4**).—A single-crystal *X*-ray analysis was undertaken of crystals of (**4**) which were grown from CH_2Cl_2 solution. The molecular structure is shown in Figure 5 and the principal interatomic distances and angles are given in Table 4. The structure is readily seen to be of the open 'boat' (**I**) ten-vertex *nido*/*arachno* type, with the selenium and platinum atoms in the 6 and 9 positions. There is a crystallographic mirror plane passing through the selenium, platinum, and boron atoms B(2) and B(4) of Figure 5; the hydrogen atoms were located from difference maps. Because of the mirror plane a number of boron atoms in (**4**) are crystallographically equivalent; B(1) ≡ B(3), B(5) ≡ B(7), and B(8) ≡ B(10), compare Figure 5 and (**I**). Data relating to only one of each of these equivalent pairs are given in Table 4.

The platinum atom has a pseudo square-planar co-ordination involving the two equivalent phosphorus atoms and the two equivalent boron atoms B(8) and B(10) (Figure 5), but it is also apparent that there is at least an equally significant interaction with B(4) as well. The distance from the platinum atom to B(4) is 2.147(10) Å and to B(8) [or B(10)] 2.230(7) Å. Similar differences have been reported in other related compounds,[5,6,16] and, as has been discussed previously,[9,10] it may be possible to invoke a strong Pt–B(4) interaction which could lead to a short platinum–boron distance. We address this topic in more detail below. In the previously reported compounds (**7**)—(**11**), and in the product of pyrolysis of (**9**), *i.e.* [9,9-$(Ph_2PC_6H_4)_2$-6,9-$CPtB_8H_{10}$] (**13**),[25] the 'short' platinum–boron distances ranged from 2.184(16) [in one determination of (**10**)][5] to 2.21(2) Å [in another determination of (**10**)],[6] with the value in (**13**) being exceptionally short at 2.08(3) Å.[25] The 'long' platinum–boron

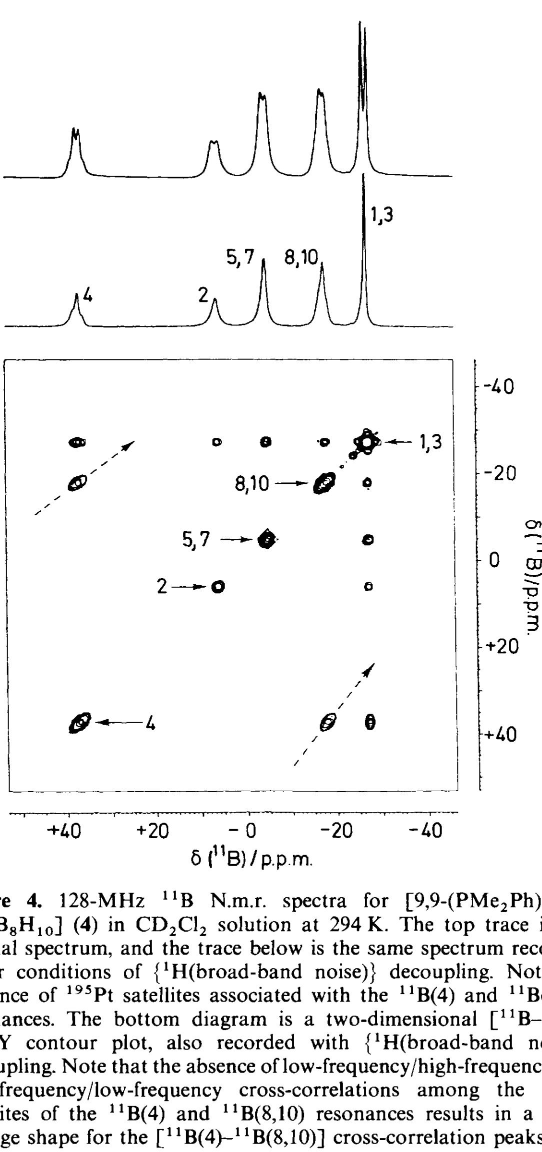

Figure 4. 128-MHz ^{11}B N.m.r. spectra for $[9,9\text{-}(PMe_2Ph)_2\text{-}6,9\text{-}SePtB_8H_{10}]$ (**4**) in CD_2Cl_2 solution at 294 K. The top trace is the normal spectrum, and the trace below is the same spectrum recorded under conditions of {^{1}H(broad-band noise)} decoupling. Note the presence of ^{195}Pt satellites associated with the ^{11}B(4) and ^{11}B(8,10) resonances. The bottom diagram is a two-dimensional [^{11}B–^{11}B]-COSY contour plot, also recorded with {^{1}H(broad-band noise)} decoupling. Note that the absence of low-frequency/high-frequency and high-frequency/low-frequency cross-correlations among the ^{195}Pt satellites of the ^{11}B(4) and ^{11}B(8,10) resonances results in a tilted lozenge shape for the [^{11}B(4)–^{11}B(8,10)] cross-correlation peaks, and that the direction of the tilt thereby indicates that the couplings $^1J(^{195}Pt\text{–}^{11}B)$ for ^{11}B(4) and ^{11}B(8,10) have the same sign (compare refs. 7 and 13)

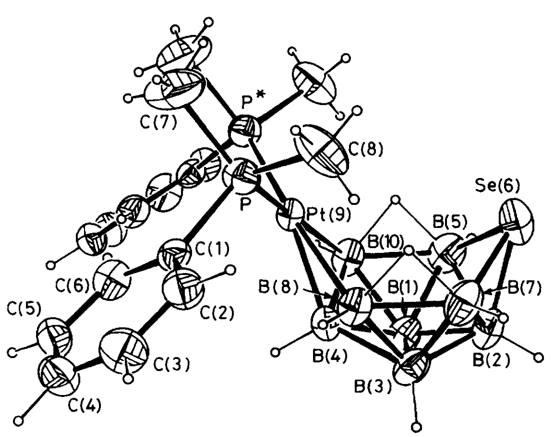

Figure 5. ORTEP plot of *arachno*-$[9,9\text{-}(PMe_2Ph)_2\text{-}6,9\text{-}SePtB_8H_{10}]$ (**4**) showing the numbering scheme used in the crystallographic analysis; ellipsoids are at the 50% level

distances in (**7**)—(**11**) and (**13**) range from 2.222(17) Å [in (**10**)][5] to 2.28(2) Å [also in (**10**)].[6] One of the values in compound (**13**), 2.17(3) Å, was found to be shorter than those in (**7**)—(**11**) and shorter than the other value in (**13**), 2.23(3) Å.[25] Another exceptionally short distance is that between platinum and the boron subtending the OEt group in (**11**), at 2.166(24) Å.[5] The B(8)–Pt–B(10) angle in (**4**) is 84.8(3)° which is very similar to the angles previously reported in (**7**)—(**11**). These range from 83.4(3)° in (**9**)[6] to 85.0(7)° in (**11**).[5] The corresponding angle in (**13**) is 87.9(11)°.[14]

The Se–B(5) distance [2.113(8) Å] is slightly longer than Se–B(2) [2.062(15) Å]. Similar effects were found in the carbaborane derivative (**9**),[6] with the shorter carbon–carbon distance being 1.64(1) [compared to 1.71(1) and 1.75(1) Å], and also in the thiaborane derivative (**11**)[5] where the analogous sulphur–boron distances are 1.91(2), 1.98(2), and 1.97(2) Å. However, for the thiaborane compound $[9,9\text{-}(PPh_3)_2\text{-}6,9\text{-}SPtB_8H_{10}]$ (**10**), where two *X*-ray studies have been performed and two sets of data reported,[5,6] Kukina *et al.*[6] gave the sulphur–boron distances as 1.94(2), 1.93(2), and 1.92(2) Å whereas Hilty *et al.*[5] gave 1.92(2), 1.96(3), and 1.92(2) Å for the same three distances. The product of the thermolysis of (**9**) has C–B distances of 1.68(4) and 1.76(4) Å respectively.[25]

Although the structure of no other *arachno*-metallaselenaborane has been reported, the selenium–boron distances in (**4**) are comparable with those in the *closo* compounds (**1**) and (**5**) and the *nido* species $[7\text{-}(\eta^5\text{-}C_5H_5)\text{-}7,8,12\text{-}CoSe_2B_9H_9]$,[26] these being 2.098(9)—2.210(6), 2.01(3)—2.20(2), and 2.004(5)—2.160(5) Å, respectively.

The interboron distances in (**4**), which are in the range of 1.746(13)—1.914(11) Å, are generally similar to those in the *closo* compounds (**1**) and (**5**). The distance between the boron atoms in the open face, *i.e.* B(5)–B(10) [or B(7)–B(8)] is 1.845(11) Å. This is considerably shorter than the corresponding values reported in ten-atom *nido*-metallaboranes, for example 1.993(16) and 1.997(16) Å in *nido*-$[6,6\text{-}(PPh_3)_2\text{-}6\text{-}H\text{-}6\text{-}IrB_9H_{13}]$[27] and 2.010(7) and 2.094(8) Å in *nido*-$[6,6,6\text{-}(PMe_2Ph)_3\text{-}6\text{-}H\text{-}6\text{-}ReB_9H_{13}]$.[28] On the other hand they are almost the same as the corresponding distances in other *arachno*-metallaboranes, for example 1.894(8) Å in *arachno*-$[6,6,9,9\text{-}(PMe_2Ph)_4\text{-}6,9\text{-}Pt_2B_8H_{10}]$).[16] In (**4**) the shortest interboron distance of 1.746(13) Å is found between B(1) [or B(3)] and B(2) while the longest, at 1.914(11) Å, is between B(2) and B(5) [or B(7)]. The co-ordinates of the bridging hydrogen atom (Figure 5) were determined from a difference map and were included (but not refined) in the least-squares refinement. The B–H (bridge) distances are both 1.40 Å.

The equivalent platinum–phosphorus bond lengths, 2.295(2) Å, are virtually the same as that of 2.304(2) Å in *arachno*-$[6,6,9,9\text{-}(PMe_2Ph)_4\text{-}6,9\text{-}Pt_2B_8H_{10}]$,[16] as perhaps expected from the similarities of their ^{195}Pt and ^{31}P n.m.r. spectra. The bond length in (**4**) is within the typical range observed for Pt–P bonds in other *nido*- and *closo*-platinaheteroboranes.[2,5–7,18] Interestingly, the P–Pt–P angle in (**4**) which the crystallographic mirror plane bisects, was determined as 103.78(6)°, somewhat larger than the corresponding angles in (**7**)—(**11**), which range from 97.7(1) in (**7**)[8] to 98.70(7)° in (**9**).[6] In the cycloboronated complex (**13**) this angle becomes 109.5(2)°,[25] but this of course will be subject to the bonding constraints imposed by the cycloboronation. The larger value in (**4**) may be associated with the eclipsed nature of the P-organyl group, and the near coplanarity of the two phenyl groups is noteworthy in this context.

Bonding of Heteroatoms in the arachno *Ten-vertex Compound* (**4**) *and Related Compounds.*—An analysis of the frontier orbitals of the platinum–phosphine and heteroborane units was undertaken in an attempt to elucidate the possible modes of

Table 4. Molecular dimensions of $[9.9\text{-}(PMe_2Ph)_2\text{-}6,9\text{-}SePtB_8H_{10}]$ (**4**);* distances in Å, angles in °

Pt(9)–P (or P*)	2.295(2)	B(5) (or 7)–B(10) (or 8)	1.845(11)
Pt(9)–B(4)	2.147(10)	B(4)–B(8) (or 10)	1.763(9)
Pt(9)–B(8) (or 10)	2.230(7)	P–C(1)	1.820(5)
Se(6)–B(2)	2.062(15)	P–C(7)	1.820(10)
Se(6)–B(5) (or 7)	2.113(8)	P–C(8)	1.826(9)
B(1)–B(3)	1.790(10)	C(1)–C(2)	1.396(8)
B(1) (or 3)–B(2)	1.746(13)	C(1)–C(6)	1.367(8)
B(1) (or 3)–B(5) (or 7)	1.757(12)	C(2)–C(3)	1.373(10)
B(1) (or 3)–B(4)	1.801(11)	C(3)–C(4)	1.371(11)
B(1) (or 3)–B(10) (or 8)	1.800(11)	C(4)–C(5)	1.382(12)
B(2)–B(5) (or 7)	1.914(11)	C(5)–C(6)	1.387(10)

P–Pt(9)–P*	103.78(6)	B(8)–B(4)–B(10)	117.0(7)
P–Pt(9)–B(4)	126.00(7)	Se(6)–B(5)–B(1)	111.8(5)
P–Pt(9)–B(8)	167.7(2)	Se(6)–B(5)–B(2)	61.4(5)
P–Pt(9)–B(10)	85.6(2)	Se(6)–B(5)–B(10)	120.9(5)
B(4)–Pt(9)–B(10)	47.5(2)	B(1)–B(5)–B(2)	56.6(5)
B(8)–Pt(9)–B(10)	84.8(3)	B(1)–B(5)–B(10)	107.1(6)
B(2)–Se(6)–B(5)	54.6(3)	Pt(9)–B(10)–B(1)	117.7(4)
B(5)–Se(6)–B(7)	91.8(3)	Pt(9)–B(10)–B(5)	117.8(4)
B(2)–B(1)–B(3)	59.2(4)	B(1)–B(10)–B(4)	60.7(5)
B(2)–B(1)–B(4)	109.8(5)	B(1)–B(10)–B(5)	57.6(4)
B(2)–B(1)–B(5)	66.2(5)	B(4)–B(10)–B(5)	106.0(5)
B(2)–B(1)–B(10)	117.0(7)	Pt(9)–P–C(1)	110.6(2)
B(3)–B(1)–B(4)	60.2(4)	Pt(9)–P–C(7)	123.4(3)
B(3)–B(1)–B(10)	109.8(5)	Pt(9)–P–C(8)	114.4(3)
B(5)–B(1)–B(3)	110.7(6)	C(1)–P–C(7)	99.7(3)
B(5)–B(1)–B(4)	108.1(6)	C(1)–P–C(8)	107.0(3)
B(5)–B(1)–B(10)	62.5(5)	C(7)–P–C(8)	99.8(4)
Se(6)–B(2)–B(1)	114.7(7)	P–C(1)–C(2)	121.7(4)
B(1)–B(2)–B(3)	61.7(5)	P–C(1)–C(6)	118.2(4)
B(1)–B(2)–B(7)	105.7(7)	C(2)–C(1)–C(6)	120.0(5)
B(5)–B(2)–B(7)	104.9(7)	C(1)–C(2)–C(3)	119.0(6)
Pt(9)–B(4)–B(1)	122.0(5)	C(2)–C(3)–C(4)	121.3(7)
Pt(9)–B(4)–B(10)	68.7(4)	C(3)–C(4)–C(5)	119.5(7)
B(1)–B(4)–B(3)	59.6(5)	C(4)–C(5)–C(6)	119.7(6)
B(1)–B(4)–B(10)	60.7(4)	C(1)–C(6)–C(5)	120.4(6)
B(3)–B(4)–B(10)	111.0(6)		

The * refers to P at equivalent position *x*,*y*,−*z*. Atom numbering as in Figure 5. B(1) ≡ B(3), B(5) ≡ B(7), and B(8) ≡ B(10), see text.

bonding. The electronic structure of the SB_8 fragment was calculated with the MNDO program,[29] and the following structures were considered: (*a*) *arachno*-$[SB_8H_{10}]^{2-}$ (**II**) calculated with free variation of all structural parameters, (*b*) *nido*-SB_8H_{10} (**III**) also calculated with free variation of all structural parameters, and (*c*) *nido*-SB_8H_{10} (**IV**) with all interatomic distances as in (**III**) except for the B(6)–B(8) distance which was changed from the value of 2.14 Å in (**III**) to 3.10 Å in order to correspond to the observed distance in (**II**). Both (**II**) and (**III**) have the gross structures of known nine-atom *arachno* or *nido* compounds such as $[B_9H_{14}]^-$,[30] $B_9H_{13}(MeCN)$,[31] 4,5-$C_2B_7H_{13}$,[32] and 4,6,8-$SC_2B_6H_{10}$[33] [compare (**II**)] and $[B_9H_{12}]^-$,[34] $C_2B_7H_9Me_2$,[35] and 7-CB_8H_{12}[36] [compare (**III**)].

We have chosen to use the same numbering scheme in (**II**)—(**IV**), *i.e.* that of an *arachno*-nine-atom system, to facilitate direct comparison of the results of the calculations. It was decided to analyse the bonding of a cationic $[PtP_2]^{2+}$ unit with anionic (**II**) and of a neutral PtP_2 unit with neutral (**III**) and (**IV**), in order to ascertain what electronic and structural features of *arachno* or *nido* ligands could be of importance in compounds like (**4**). The following discussion focuses on the possible interactions between the B_3 face of the heteroborane unit which bonds to the platinum atom and the *d*-based orbitals of the $[PtP_2]^{2+}$ or PtP_2 units. It has been established that the PtP_2 unit has the orbital sequence shown in Figure 6(*a*).[37] The orbitals are labelled for convenience according to their *d* component and to the C_{2v}-based symmetry label associated with the PtP_2 unit located in the Cartesian system shown in Figure 6(*b*). Although the energies of the orbitals in the $[PtP_2]^{2+}$ unit do not appear to have been reported, it is expected that the two electrons removed from the PtP_2 unit will be those from the d_{yz} orbital and hence the unfilled d_{z^2} and d_{yz} orbitals will be well separated from the other *d* orbitals.

Before discussing the nature of the interactions of *arachno*-$[SB_8H_{10}]^{2-}$ (**II**) and $[PtP_2]^{2+}$, it should be noted that the calculated structure of (**II**) contains all the expected features of such an *arachno*-nine-vertex cluster. The distances between sulphur and the adjacent boron atoms were very similar [S to B(5,9) 1.86 Å and S to B(1) 1.84 Å], and the interboron distance between B(5) and B(9) was 2.80 Å. There were no bridging hydrogen atoms but there were two BH_2 groups at the (6) and (8) positions with *endo*-hydrogen atoms.

An analysis of the frontier orbitals of (**II**) and $[PtP_2]^{2+}$ clearly shows that there are three interactions of major importance. Two of these involve filled orbitals on (**II**) [the h.o.m.o. and h.o.m.o. − 2] and empty orbitals on $[PtP_2]^{2+}$ [d_{z^2} and d_{yz} respectively], and the third interaction is between the l.u.m.o. of (**II**) and the d_{xz} (possibly h.o.m.o.) on the platinum unit. Figures 7(*a*)—(*c*) illustrate these combinations and detail the percentage contributions of the orbitals on the B_3 face of (**II**). The interaction shown in Figure 7(*a*) involves each boron atom of the B_3 face approximately equally and does not in itself lead to the observed conformation of the PtP_2 unit with respect to the B_3 face. This conformation is a result of the interactions shown in Figure 7(*b*) and (*c*). As shown in Figure 7(*b*), d_{yz} on platinum interacts strongly with the B_3 face [25% on B(6/8), 23% on B(7)], and also, as shown in Figure 7(*c*), a filled orbital on platinum (d_{xz}) interacts with the l.u.m.o. of (**II**) [37% on B(7), 8% on the two *endo* terminal H atoms]. This therefore also contributes to the conformation of the $[PtP_2]^{2+}$ unit. In sum, the $[PtP_2]^{2+}$ unit may be regarded as a formal two-electron cluster contributor in this context, *i.e.* neutral PtP_2 would be a four-electron unit and (**4**) would be an *arachno* cluster. Bonding the $[PtP_2]^{2+}$ unit to (**II**) would cause a relocation of the *endo* B–H atoms probably to semi-bridging or bridging positions as in (**4**) or $[B_{10}H_{14}]^{2-}$.[23] These hydrogen atoms were not located in the *X*-ray analysis of (**4**) but in $[9,9\text{-}(PPh_3)_2\text{-}6,9\text{-}CPtB_8H_{12}]$ they were found asymmetrically bridging with the mean μ-H-B (adjacent to Pt) distance 1.08(10) Å, shorter than the mean μ-H-B (adacent to C) distance 1.32(3) Å.[6] Note in this context that n.m.r. spectroscopy (see above) shows that there is bonding asymmetry to these bridging hydrogen atoms in compound (**4**).

Just as (**II**) was consistently *arachno*, the calculated structure for *nido*-SB_8H_{10} (**III**) contained all the expected features for the *nido* formulation. The distances between sulphur and the adjacent boron atoms are S to B(5/9) 1.85 Å and S to B(1) 1.86 Å and the interboron distance B(5) to B(9) is 2.80 Å compared to 2.14 Å between B(6) and B(8). The bridging hydrogen atoms are closer to B(6/8), 1.29 Å, than B(5/9), 1.46 Å. The results of the m.o. calculation suggest that the interaction of the PtP_2 unit with the B_3 face of (**III**) would occur mainly through the combination of the h.o.m.o. of PtP_2 and l.u.m.o. of (**III**) which is 23% located on the B_3 face, but there is also the possibility of this platinum orbital interacting with another unfilled orbital (l.u.m.o. + 3) on B_3 (19%) which is 1.4 eV higher in energy. Additionally, the l.u.m.o. of the PtP_2 unit can interact with either the h.o.m.o. − 1 or the h.o.m.o. − 3 of (**III**). These two orbitals are 0.3 and 0.8 eV more stable than the h.o.m.o. and are located on the B_3 face to the extent of 14 and 23% respectively. Compared to the previous case however, the possibility of extra electron density being incorporated into the metallaheteroboranes from the metal by means of interactions involving the $d_{x^2-y^2}$, d_{xy}, or d_{xz} orbitals appears extremely unlikely. There is only one unfilled orbital on (**III**) (l.u.m.o. + 6) (2.3 eV above

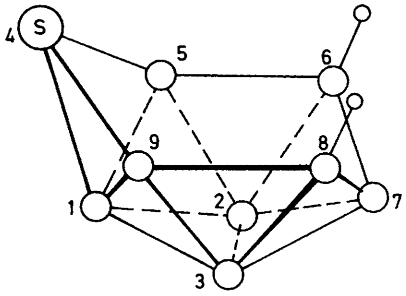

(II)

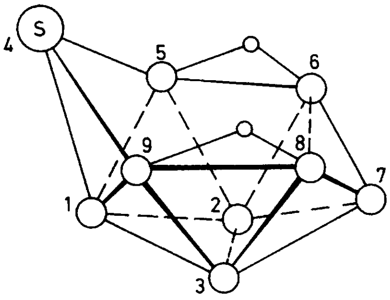

(III)

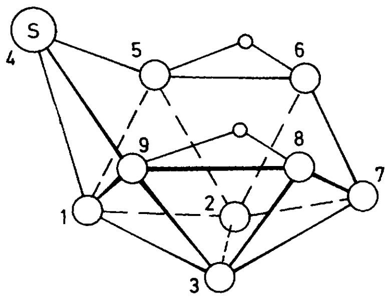

(IV)

the l.u.m.o. and 36% located on B_3), in the section of orbitals from the l.u.m.o. to the l.u.m.o. +11 (covering 4.9 eV) which could interact. Moreover the l.u.m.o. +6 orbital could only interact with the $d_{x^2-y^2}$ orbital on platinum and the geometry of this interaction would preclude an efficient interaction. Hence, in general terms, the neutral PtP_2 unit could only interact with **(III)** as a two-electron cluster unit.

Breaking the B(6)–B(8) bond in **(III)** to produce SB_8H_{10} with structure **(IV)** appears to have relatively minor overall effects, in terms of these calculations, on the bonding interactions just described. Both the interaction between the PtP_2 unit h.o.m.o. and the SB_8H_{10} l.u.m.o. [30% on B(6) and B(8) of B_3] and that between the PtP_2 unit l.u.m.o. and the SB_8H_{10} h.o.m.o. (49% on B_3) are more localised and more significant, but no other interaction involving either the PtP_2 h.o.m.o. or l.u.m.o. emerges. Furthermore, the interaction involving $d_{x^2-y^2}$ is even less significant in the combination of **(IV)** and PtP_2 than **(III)** and PtP_2 since the orbital on **(IV)** is higher in energy (3.2 eV above the l.u.m.o.) and only 31% based on the B_3 face.

Thus comparison of the interactions involving **(II)**—**(IV)** discussed above clearly shows that the PtP_2 unit could only interact effectively as a four-electron cluster unit with a ligand which has an *arachno* structure and furthermore that such interactions appear to be highly sensitive to details of structure. We consider compound **(4)** to be best classified as of the *arachno* type because of the evidence deriving from the cluster geometry and n.m.r. spectroscopy.

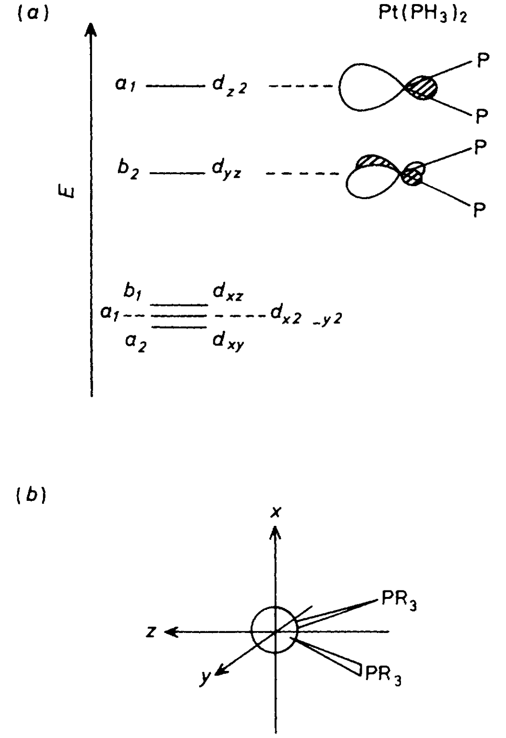

Figure 6. (*a*) Energy-level diagram of the frontier orbitals of the $Pt(PH_3)_2$ fragment labelled to show the *d*-orbital components. (*b*) The PtP_2 unit located in the Cartesian system used in the discussion of the bonding in compound (**4**)

It is noteworthy that in all the combinations of thiaborane ligands and platinum–phosphine units considered above the conformation of the PtP_2 unit with respect to the B_3 face is the same. Moreover, this conformation is found in all the structures of PtP_2-containing $XPtB_8$ compounds which have been reported. A similar analysis of the conformation of other units such as CH_2 (or BH_2^- of BHL) in a 6 or 9 position can be produced. In these cases the interactions that determine the conformation occur between the b_1 l.u.m.o. of CH_2 [38] and filled orbitals on the heteroborane ligands. Because the b_1 orbital on quasi-tetrahedral CH_2 [39] is orientated at 90° to the b_2 orbital on the quasi-square-planar PtP_2 unit [Figure 6(*a*)] the conformations of these groups are at 90° to each other.

The bonding of the sulphur atom in **(II)**—**(IV)** is essentially the same in each species and closely related to that in *closo*-1-SB_9H_9.[38] The calculated localised picture of the bonding about sulphur shows that two electrons occupy a non-directional, 'lone pair', *s* orbital on sulphur and there are three two-centre S–B bonds to the adjacent boron atoms in the borane fragment. There is a small positive charge located at the sulphur atom in the ligands **(II)**—**(IV)** which ranges from 0.21 in **(II)** to 0.38 in **(IV)**. In general terms the S atom can be considered as equivalent to $[BH]^{2-}$ providing four electrons and three orbitals for cluster bonding.

Experimental

The compounds *cis*-$[PtCl_2(PEt_3)_2]$ and *cis*-$[PtCl_2(PMe_2Ph)_2]$ were prepared by literature methods[40,41] as were the $[NEt_4]^+$ and $[NHEt_3]^+$ salts of $[7\text{-}SeB_{10}H_{11}]^-$.[42] The complex *cis*-$[PtCl_2(PBu^n{}_3)_2]$ was obtained from the Aldrich Chemical Co. or Strem Chemicals Inc. and used as supplied. All experiments

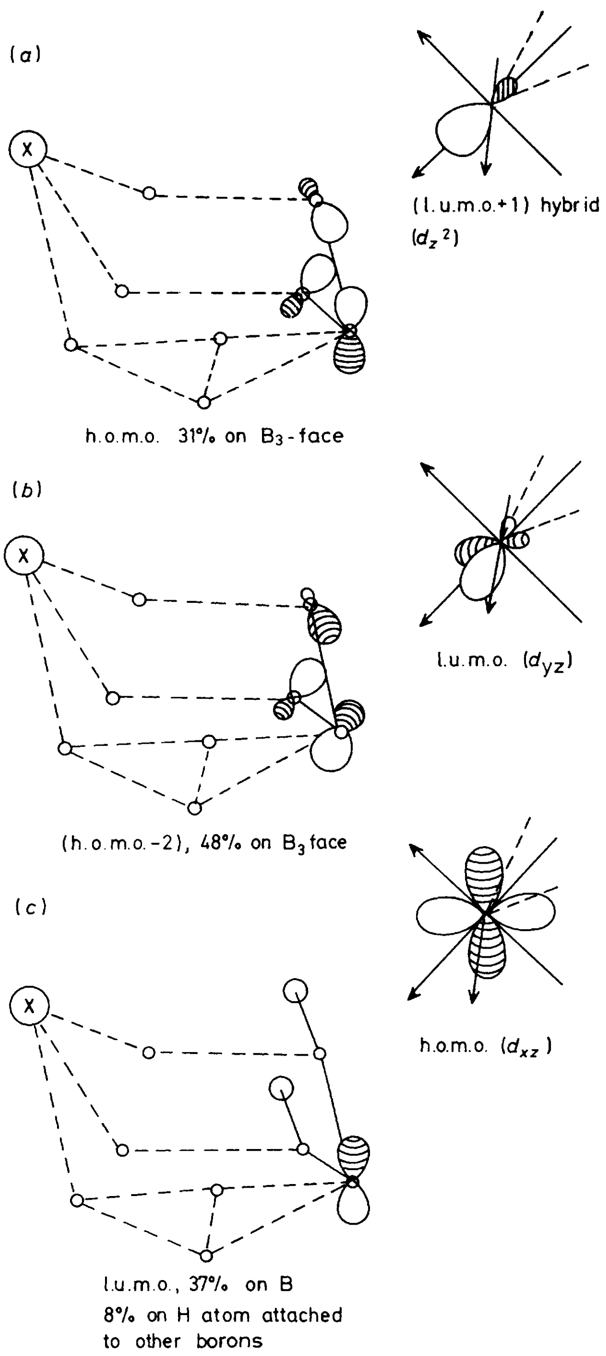

Figure 7. Frontier-orbital interactions between (**II**) and $[PtP_2]^{2+}$: (*a*) the (**II**) h.o.m.o.–$[PtP_2]^{2+}$ (l.u.m.o. + 1) interaction; (*b*) the (**II**) (h.o.m.o.–2)–$[PtP_2]^{2+}$ l.u.m.o. interaction; (*c*) the (**II**) l.u.m.o.–$[PtP_2]^{2+}$ h.o.m.o. interaction

were carried out under inert gas. I.r. spectra were recorded as KBr discs on Perkin-Elmer 457, 682, and 1 310 spectrometers.

Reaction of $[NHEt_3][7\text{-}SeB_{10}H_{11}]$ *with* cis-$[PtCl_2(PEt_3)_2]$.—A suspension of *cis*-$[PtCl_2(PEt_3)_2]$ (0.400 g, 0.80 mmol) in thf (20 cm^3) was added to a solution of $[NHEt_3][7\text{-}SeB_{10}H_{11}]$ (0.239 g, 0.80 mmol) in thf (20 cm^3). The yellow colour immediately changed to orange-yellow. After stirring at room temperature for 4 d the reaction mixture was filtered. Removal of the solvent under reduced pressure (rotary evaporator, 25 °C) yielded an orange solid. Preparative t.l.c. with CH_2Cl_2–light petroleum (b.p. 40—60 °C) (6:1) as eluant gave at least seven bands, the major one being extracted as a yellow oil which solidified on standing. Recrystallisation from CH_2Cl_2–hexane afforded orange crystals (0.06 g, 12%) of *closo*-$[2,2\text{-}(PEt_3)_2\text{-}1,2\text{-}SePtB_{10}H_{10}]$ (**1**) (Found: C, 22.3; H, 6.4. $C_{12}H_{40}B_{10}P_2PtSe$ requires C, 22.9; H, 6.4%). I.r. spectrum: $\nu_{max.}$ at 2 960m, 2 925m, 2 870m, 2 560s (BH), 2 540w (BH), 2 520vs (BH), 2 490w (BH), 1 448m, 1 415m, 1 375m, 1 270w, 1 247m, 1 038s, 1 030s, 1 010s, 940w, 920m, 900w, 880w, 820vw, 765vs, 720vs, 670w, and 632m cm^{-1}. N.m.r. data in Table 1.

X-Ray Analysis of $[(PEt_3)_2PtSeB_{10}H_{10}]$ (**1**).—*Crystal data.* $C_{12}H_{40}B_{10}P_2PtSe$, $M = 628.56$, orthorhombic, $a = 55.052(6)$, $b = 17.842(5)$, $c = 10.259(4)$ Å, $U = 10\,076(4)$ Å^3, $Z = 16$, $D_c = 1.66$ g cm^{-3}, $F(000) = 4\,864$, $\lambda(\text{Mo-}K_\alpha) = 0.710\,73$ Å, $\mu(\text{Mo-}K_\alpha) = 71.8$ cm^{-1}, space group *Fdd*2 (no. 43) uniquely from the systematic absences $hkl, h + k, k + l, (l + h) = 2n + 1$; $0kl, k + l = 4n + 1$; $h0l, l + h = 4n + 1$.

Structure determination. A crystal of dimensions 0.55 × 0.25 × 0.06 mm was used for data collection. Accurate cell dimensions and the crystal orientation matrix were determined on an Enraf–Nonius CAD-4 diffractometer by least-squares treatment of the setting angles of 25 reflections in the range $10 < \theta < 13°$. Intensities of reflections with indices *h* 0—70, *k* 0—22, *l* 0—13 were measured with data collected in the range $2 < 2\theta < 54°$ by the ω—2θ scan method; ω scan width (0.70 + 0.35 tanθ) with graphite-monchromatized Mo-K_α radiation. The intensities of three reflections measured every 2 h showed no evidence of crystal decay. A total of 3 188 reflections were measured of which 2 896 were unique; the 2 251 with $I > 3\sigma(I)$ were labelled observed and used in the structure solution and refinement. Data were corrected for Lorentz, polarisation, and absorption effects (maximum and minimum transmission factors 0.653 and 0.188). The co-ordinates of the Pt atom were deduced from a Patterson map; the remaining non-hydrogen atoms were located in succeeding Fourier difference syntheses. Hydrogen atoms were visible in difference maps and were included (as riding atoms C–H 0.95, B–H 1.08 Å) in the structure-factor calculations. The final cycles of full-matrix least-squares calculations with anisotropic thermal parameters included 234 variables and converged with $R = 0.042$, $R' = 0.052$, goodness-of-fit 1.30, and maximum shift/error ratio 0.02. Weights were derived from the counting statistics $w = 1/(\sigma^2F_o + 0.070F_o^2)$. The final difference map had peaks 2.4 e Å^{-3} adjacent to Pt; there were no chemically significant features. With the direction of the polar axis reversed refinement converged with higher R and R' values (0.046 and 0.057 respectively). Scattering factors and anomalous dispersion corrections were taken from ref. 43. All calculations were performed on a PDP11/73 computer using the SDP-Plus suite of programs.[44] Atomic co-ordinates and details of molecular geometry are in Tables 5 and 2 respectively. Figure 3 was prepared using ORTEP II.[45]

Additional material available from the Cambridge Crystallographic Data Centre comprises H-atom co-ordinates and thermal parameters.

Reaction of $[NEt_4][7\text{-}SeB_{10}H_{11}]$ *with* cis-$[PtCl_2(PBu^n{}_3)_2]$.—A solution of $[NEt_4][7\text{-}SeB_{10}H_{11}]$ (0.147 g, 0.45 mmol) and NEt_3 (0.091 g, 0.9 mmol) in thf (12 cm^3) was refluxed for 15 min. Upon cooling, a solution of *cis*-$[PtCl_2(PBu^n{}_3)_2]$ (0.300 g, 0.45 mmol) in thf (10 cm^3) was added. The reaction mixture was refluxed for 10 min, then allowed to cool. The solvent was removed under reduced pressure (rotary evaporator, 25 °C) giving an orange-brown solid. Preparative t.l.c. (eluant CH_2Cl_2) yielded five bands, the major one appearing as a yellow band. Recrystallisation from CH_2Cl_2–EtOH afforded yellow needles (0.125 g, 49%) of *closo*-$[2,2\text{-}(PBu^n{}_3)_2\text{-}1,2\text{-}SePtB_{10}H_{10}]$ (**2**) (Found: C, 35.6; H, 8.0.

Table 5. Positional parameters with estimated standard deviations (e.s.d.s) for compound (**1**)

Atom	*x*	*y*	*z*	Atom	*x*	*y*	*z*
Pt	0.066 27(1)	−0.188 25(3)	0.0*	C(24)	0.000 1(4)	−0.186(1)	−0.104(3)
Se	0.109 87(3)	−0.234 57(9)	0.082 3(2)	C(25)	0.030 4(4)	−0.347(1)	−0.062(2)
P(1)	0.073 71(8)	−0.090 2(2)	−0.142 5(5)	C(26)	0.015 5(4)	−0.396(1)	−0.142(3)
P(2)	0.043 67(7)	−0.263 5(2)	−0.137 6(5)	B(3)	0.075 8(3)	−0.290 3(9)	0.130(2)
C(11)	0.106 2(3)	−0.081 0(8)	−0.184(2)	B(4)	0.100 8(4)	−0.282(1)	0.261(2)
C(12)	0.116 4(4)	−0.152(1)	−0.247(3)	B(5)	0.111 0(4)	−0.186(1)	0.266(2)
C(13)	0.066 3(4)	0.001 4(8)	−0.070(2)	B(6)	0.092 6(3)	−0.128(1)	0.137(2)
C(14)	0.040 4(5)	0.014(1)	−0.051(3)	B(7)	0.050 9(3)	−0.228(1)	0.189(2)
C(15)	0.059 0(4)	−0.084(1)	−0.301(2)	B(8)	0.069 8(4)	−0.281(1)	0.296(2)
C(16)	0.064 2(5)	−0.017(1)	−0.381(3)	B(9)	0.090 6(4)	−0.220(1)	0.377(2)
C(21)	0.059 1(4)	−0.302 1(9)	−0.282(2)	B(10)	0.086 2(4)	−0.129(1)	0.311(2)
C(22)	0.080 1(4)	−0.354(1)	−0.246(3)	B(11)	0.061 3(3)	−0.133(1)	0.196(2)
C(23)	0.016 3(3)	−0.220(1)	−0.207(3)	B(12)	0.061 5(4)	−0.189(1)	0.338(2)

* The *z* co-ordinate of Pt was held at 0.0 to define the origin.

Table 6. Positional parameters with estimated standard deviations (e.s.d.s) for compound (**4**)

Atom	*x*	*y*	*z*
Pt(9)	0.0000*	0.084 58(2)	0.0
Se(6)	0.056 2(2)	−0.310 0(1)	0.0
P	0.150 0(2)	0.180 3(2)	0.103 71(9)
C(1)	−0.023 3(8)	0.270 8(5)	0.162 3(3)
C(2)	−0.040 5(8)	0.248 1(7)	0.241 2(4)
C(3)	−0.169 0(12)	0.322 9(8)	0.282 8(4)
C(4)	−0.278 8(11)	0.419 8(6)	0.248 7(5)
C(5)	−0.258 0(10)	0.444 3(7)	0.171 0(4)
C(6)	−0.131 3(10)	0.367 8(7)	0.128 0(4)
C(7)	0.337 1(13)	0.306 4(10)	0.095 1(5)
C(8)	0.272 3(14)	0.062 5(9)	0.167 0(5)
B(4)	−0.280 5(15)	−0.005 8(10)	0.0
B(10)	−0.156 6(12)	−0.038 6(8)	0.086 3(4)
B(3)	−0.329 7(13)	−0.157 5(8)	0.051 4(4)
B(5)	−0.110 3(13)	−0.219 4(8)	0.087 1(4)
B(2)	−0.240 1(21)	−0.293 3(12)	0.0

* The *x* co-ordinate was fixed to define the origin.

$C_{24}H_{64}B_{10}P_2PtSe$ requires C, 36.2; H, 8.1%). I.r. spectrum: $\nu_{max.}$ 2 955s, 2 925s, 2 860m, 2 560s (BH), 2 520s (BH), 1 460m, 1 415w, 1 375w, 1 340w, 1 300w, 1 205w, 1 090m, 1 050w, 1 010m, 970w, 908s, 795w, 770w, and 723m, cm^{-1}. N.m.r. data in Table 1.

Reaction of $[NHEt_3][7\text{-}SeB_{10}H_{11}]$ *with* $[PtCl_2(PMe_2Ph)_2]$.—A solution of $[NHEt_3][7\text{-}SeB_{10}H_{11}]$ (0.101 g, 0.336 mmol) in thf (25 cm^3) was added to a suspension of $[PtCl_2(PMe_2Ph)_2]$ (0.182 g, 0.336 mmol) in thf (25 cm^3). An immediate colour change from yellow to orange-yellow was observed. The mixture was stirred for 7 d and then refluxed for 6 h. The solvent was removed under reduced pressure (rotary evaporator, 25 °C) to yield an orange solid. Preparative t.l.c. (eluant CH_2Cl_2) gave seven bands of which only the two top bands were of significance. The topmost band was extracted into CH_2Cl_2 from which colourless crystals (53 mg, 24.4%) of $[9,9\text{-}(PMe_2Ph)_2\text{-}6,9\text{-}SePtB_8H_{10}]$ (**4**) were isolated. This compound was identified spectroscopically and by a single crystal *X*-ray analysis. I.r. spectrum: $\nu_{max.}$ 3 065w, 3 050w, 3 005w, 2 960w, 2 900w, 2 840w, 2 550s (BH), 2 530s (BH), 2 515w (BH), 2 495s (BH), 2 455s (BH), 1 570w, 1 470s, 1 430s, 1 420w, 1 400w, 1 380w, 1 320w, 1 300s, 1 285s, 1 175w, 1 155w, 1 100s, 1 070w, 1 030s, 990s, 980w, 970w, 950s, 940w, 935w, 920s, 910w, 905vs, 865s, 840s, 795s, 745s, 735w, 710s, 690s, and 680w cm^{-1}. N.m.r. data in Table 3.

The second band was also extracted into CH_2Cl_2 and gave yellow crystals (17 mg, 7.6%) of $[2,2\text{-}(PMe_2Ph)_2\text{-}1,2\text{-}SePtB_{10}H_{10}]$ (**3**) which was identified spectroscopically. I.r. spectrum: $\nu_{max.}$ 3 070w, 3 040w, 2 975w, 2 910w, 2 550s (BH), 2 505vs (BH), 2 485w (BH), 1 485w, 1 470w, 1 430s, 1 415w, 1 405w, 1 305w, 1 295w, 1 285w, 1 175w, 1 155w, 1 100s, 1 070w, 1 010s, 945s, 905vs, 860w, 840w, 770w, 740s, 710s, 690s, and 680w cm^{-1}. N.m.r. data in Table 1.

X-Ray Analysis of $[(PMe_2Ph)_2PtSeB_8H_{10}]$ (**4**).—*Crystal data.* $C_{16}H_{32}B_8P_2PtSe$, *M* = 646.92, orthorhombic, *a* = 6.935(1), *b* = 10.048(2), *c* = 17.413(2) Å, *U* = 1 213.4(7) Å^3, *Z* = 2, D_c = 1.77 g cm^{-3}, *F*(000) = 620, λ(Mo-K_α) = 0.710 73 Å, μ(Mo-K_α) = 74.5 cm^{-1}. The systematic absences (*h*0*l*, *h* + *l* = 2*n* + 1) indicate the space group to be either $P2_1nm$ or *Pmnm*. With *Z* = 2, the former requires the molecule to have mirror symmetry whereas the latter would require molecule *mm* symmetry; $P2_1nm$ was chosen and confirmed by the successful refinement.

Structure determination. A crystal of dimensions 0.37 × 0.42 × 0.48 mm was used for data collection. Accurate cell constants and the crystal orientation matrix were determined as above for (**1**) using 25 reflections in the range $10 < \theta < 15°$. Intensities of reflections with indices *h* 0—8, *k* 0—12, *l* 0—22 were measured with data collected in the range $2 < 2\theta < 54°$ by the ω—2θ scan method; ω scan width (0.60 + 0.35 tanθ) with graphite-monochromatised Mo-K_α radiation. Crystal stability was checked as for (**1**); no decay correction was applied. A total of 1 980 reflections were measured of which 1 474 were unique; those 1 375 with $I > 3\sigma(I)$ were labelled observed and used in the structure solution and refinement. Lorentz, polarisation, and absorption corrections were applied to the data (maximum and mininum transmission factors 0.42 and 0.14). The Pt and Se atoms were located from a Patterson map; the remaining non-hydrogen atoms were located in succeeding Fourier difference syntheses. Hydrogen atoms were clearly located in difference maps calculated at various stages of the refinement process. With the exception of the unique bridging hydrogen (which was included at the position found in a difference map) the hydrogens were included as riding atoms as in (**1**). The final cycles of refinement included 133 variable parameters and converged with *R* = 0.022, *R′* = 0.028, goodness-of-fit 0.93, and maximum shift/error ratio less than 0.005. In this polar space group, refinement with the direction of the polar axis reversed converged with a higher *R* value (0.030, *R′* 0.039). The final difference map had peaks ±2 e Å^{-3} adjacent to the Pt, but no chemically significant features. Weights used in the full-matrix least-squares calculations were $w = 1/(\sigma^2F_o + 0.055F_o^2)$. Scattering factors and anomalous dispersion corrections were taken from ref. 43. All calculations were performed on a PDP 11/73 computer using the SDP-Plus suite of programs.[44] Atomic co-ordinates and details of the molecular architecture are in Tables 6 and 4 respectively. Figure 5 was prepared using ORTEP II.[45]

N.M.R. Spectroscopy.—N.m.r. spectroscopy was performed at 9.4 T using commercially available instrumentation. The basic techniques of $^{1}\text{H-}\{^{11}\text{B}\}$,[8,19,20,46] $^{1}\text{H-}\{^{31}\text{P}\}$,[47] $[^{11}\text{B-}^{11}\text{B}]$-COSY,[48,49] and $[^{1}\text{H-}^{1}\text{H}]$-COSY[50,51] n.m.r. spectroscopy as used in this work were essentially as described elsewhere.[1,7] In the $^{1}\text{H-}\{^{11}\text{B}\}$ experiments use was made of the procedure[52] in which a $^{1}\text{H-}\{^{11}\text{B(off resonance)}\}$ spectrum was subtracted from a $^{1}\text{H-}\{^{11}\text{B(on resonance)}\}$ spectrum in order to remove proton resonances not coupled to the ^{11}B nucleus of interest. Additionally, in the $^{1}\text{H-}\{^{11}\text{B(selective)}\}$ work among the ^{195}Pt satellites, clarification was often achieved by subtraction among ^{1}H spectra obtained with decoupling at $\nu(^{11}\text{B})$, $\nu(^{11}\text{B}) + \frac{1}{2}J(^{195}\text{Pt-}^{11}\text{B})$, and $\nu(^{11}\text{B}) - \frac{1}{2}J(^{195}\text{Pt-}^{11}\text{B})$. In the $[^{11}\text{B-}^{11}\text{B}]$-COSY and $[^{1}\text{H-}^{1}\text{H}]$-COSY experiments $\{^{1}\text{H(broad-band noise)}\}$ and $\{^{11}\text{B(broad-band noise)}\}$ decoupling respectively were applied continuously. Typical experimental parameters for the types of COSY experiments used in this work are summarised in ref. 7. Other spectroscopy was straightforward, relaxation times $T_1(^{11}\text{B})$ being measured by the inversion-recovery method, and chemical shifts δ being quoted positive to high frequency (low field) of Ξ 100 for ^{1}H, 40.480 730 (nominally 85% H_3PO_4) for ^{31}P, and 32.083 971 MHz [nominally $BF_3(OEt_2)$ in $CDCl_3$] for ^{11}B (Ξ is defined in ref. 53). The activation energy $\Delta G^{\ddagger}$ for the fluxionality of compound (**3**) was measured in CD_2Cl_2 solution by observing the coalescence temperature, in the $^{1}\text{H-}\{^{31}\text{P(broad-band noise)}\}$ spectrum, of the two proton resonances arising from the two chemically inequivalent types of P-methyl group (Table 1, footnote *p*).

Acknowledgements

A generous loan of platinum salts from Johnson-Matthey plc is gratefully acknowledged. G. F. thanks the National Science and Engineering Research Council Canada for Grants in Aid of Research, X. L. R. F. and J. D. K. thank the S.E.R.C. of the United Kingdom for facilities, Faridoon and O. Ni D. thank the Department of Education of the Republic of Ireland for Studentships, and T. R. S., J. D. K., and X. L. R. F. thank Professor N. N. Greenwood for his encouragement.

References

1 Part 4, Faridoon, O. Ni Dhubhghaill, T. R. Spalding, G. Ferguson, B. Kaitner, X. L. R. Fontaine, J. D. Kennedy, and D. Reed, *J. Chem. Soc., Dalton Trans.*, 1988, 2739.
2 G. Ferguson, M. Parvez, J. A. MacCurtain, O. Ni Dhubhghaill, T. R. Spalding, and D. Reed, *J. Chem. Soc., Dalton Trans.*, 1987, 699.
3 W. R. Hertler, F. Klanberg, and E. L. Muetterties, *Inorg. Chem.*, 1967, **6**, 1696; A. R. Kane, L. J. Guggenberger, and E. L. Muetterties, *J. Am. Chem. Soc.*, 1970, **92**, 2571.
4 A. R. Siedle, D. McDowell, and L. J. Todd, *Inorg. Chem.*, 1974, **13**, 2735.
5 T. K. Hilty, D. A. Thompson, W. M. Butler, and R. W. Rudolph, *Inorg. Chem.*, 1979, **18**, 2642.
6 G. A. Kukina, M. A. Porai-Koshits, V. S. Sergienko, Yu. V. Zefirov, and G. G. Sadikov, *Koord. Khim.*, 1985, **11**, 385.
7 G. Ferguson, J. D. Kennedy, X. L. R. Fontaine, Faridoon, and T. R. Spalding, *J. Chem. Soc., Dalton Trans.*, 1988, 2555.
8 Y. M. Cheek, N. N. Greenwood, J. D. Kennedy, and W. S. McDonald, *J. Chem. Soc., Chem. Commun.*, 1982, 80.
9 A. J. Welch, *J. Chem. Soc., Dalton Trans.*, 1975, 2270.
10 M. Green, J. L. Spencer, F. G. A. Stone, and A. J. Welch, *J. Chem. Soc., Dalton Trans.*, 1975, 179.
11 A. J. Welch, *J. Chem. Soc., Dalton Trans.*, 1975, 1473.
12 E. W. Corcoran and L. G. Sneddon, *Inorg. Chem.*, 1985, **107**, 7446 and refs. therein.
13 M. A. Beckett, J. D. Kennedy, and O. W. Howarth, *J. Chem. Soc., Chem. Commun.*, 1985, 855.
14 J. D. Kennedy and B. Wrackmeyer, *J. Magn. Reson.*, 1980, **38**, 529.
15 N. N. Greenwood, M. J. Hails, J. D. Kennedy, and W. S. McDonald, *J. Chem. Soc., Dalton Trans.*, 1985, 953.
16 S. K. Boocock, N. N. Greenwood, M. J. Hails, J. D. Kennedy, and W. S. McDonald, *J. Chem. Soc., Dalton Trans.*, 1981, 1415.
17 J. Bould, N. N. Greenwood, and J. D. Kennedy, *J. Chem. Soc., Dalton Trans.*, 1984, 2477.
18 J. D. Kennedy, *Prog. Inorg. Chem.*, 1986, **34**, 211 and refs. therein.
19 M. A. Beckett and J. D. Kennedy, *J. Chem. Soc., Chem. Commun.*, 1983, 275.
20 J. D. Kennedy, in 'Multinuclear N.M.R.,' ed. J. Mason, Plenum, London, New York, 1987, ch. 8, pp. 221—254 and refs. therein.
21 K. Baše, A. Petrina, B. Štíbr, V. Petricek, K. Malý, A. Linek, and I. A. Zakharova, *Chem. Ind. (London)*, 1979, 212.
22 B. Štíbr, S. Heřmánek, J. Plešek, K. Baše, and I. A. Zakharova, *Chem. Ind. (London)*, 1980, 468.
23 D. S. Kendall and W. N. Lipscomb, *Inorg. Chem.*, 1973, **12**, 546.
24 V. R. Brill, H. Dietrick, and H. Dierks, *Acta Crystallogr., Sect. B*, 1971, **27**, 2003.
25 G. A. Kukina, S. V. Sergienko, M. A. Porai-Koshits, K. Baše, and I. A. Zakharova, *Izv. Acad. Nauk. S.S.S.R., Ser. Khim.*, 1981, **12**, 2838.
26 G. D. Friesen, A. Barriola, D. Daluga, P. Ragatz, J. C. Huffman, and L. J. Todd, *Inorg. Chem.*, 1980, **19**, 458.
27 S. K. Boocock, J. Bould, N. N. Greenwood, J. D. Kennedy, and W. S. McDonald, *J. Chem. Soc., Dalton Trans.*, 1982, 713.
28 M. A. Beckett, N. N. Greenwood, J. D. Kennedy, and M. Thornton-Pett, *J. Chem. Soc., Dalton Trans.*, 1985, 1119.
29 M. J. S. Dewar and W. Thiel, *J. Am. Chem. Soc.*, 1977, **99**, 2531; W. Thiel, Quantum Chemistry Program Exchange, Indiana State University, Bloomington, 1978, vol. 11, p. 353.
30 N. N. Greenwood, J. A. McGinnety, and J. D. Owen, *J. Chem. Soc., Dalton Trans.*, 1972, 986.
31 F. E. Wang, P. G. Simpson, and W. N. Lipscomb, *J. Am. Chem. Soc.*, 1961, **83**, 491.
32 T. Jelínek, B. Štíbr, F. Mares, J. Plešek, and S. Heřmánek, *Polyhedron*, 1987, **6**, 1737.
33 K. Baše, S. Heřmánek, and F. Hanousek, *J. Chem. Soc., Chem. Commun.*, 1984, 299.
34 G. B. Jacobsen, D. G. Meina, J. H. Morris, C. Thomson, S. J. Andrews, D. Reed, A. J. Welch, and D. F. Gaines, *J. Chem. Soc., Dalton Trans.*, 1985, 1645.
35 J. C. Huffman and W. E. Streib, *J. Chem. Soc., Chem. Commun.*, 1972, 665.
36 S. Heřmánek, J. Fusek, B. Štíbr, J. Plešek, and T. Jelínek, *Polyhedron*, 1986, **5**, 1873.
37 D. G. Evans and D. M. P. Mingos, *J. Organomet. Chem.*, 1982, **240**, 321.
38 J. A. MacCurtain, P. Brint, and T. R. Spalding, *J. Chem. Soc., Dalton Trans.*, 1985, 2591.
39 W. J. Hehre, L. Radom, P. v. R. Schleyer, and J. A. Pople, 'Ab initio Molecular Orbital Theory,' Wiley, New York, 1985.
40 G. W. Parshall, *Inorg. Synth.*, 1970, **12**, 27.
41 G. B. Kauffman and D. O. Cowan, *Inorg. Synth.*, 1960, **6**, 211.
42 J. L. Little, G. D. Friesen, and J. L. Todd, *Inorg. Chem.*, 1977, **16**, 869.
43 'International Tables for *X*-ray Crystallography,' Kynoch Press, Birmingham, 1974, vol. 4.
44 SDP-Plus, B. Frenz and Associates Inc., College Station, Texas 77840, and Enraf–Nonius, Delft, 1983.
45 C. K. Johnson, ORTEP II, Report ORNL-5138, Oak Ridge National Laboratory, Tennessee, 1976.
46 X. L. R. Fontaine and J. D. Kennedy, *J. Chem. Soc., Dalton Trans.*, 1987, 1573.
47 S. K. Boocock, N. N. Greenwood, J. D. Kennedy, W. S. McDonald, and J. Staves, *J. Chem. Soc., Dalton Trans.*, 1981, 2573.
48 M. Bown, X. L. R. Fontaine, and J. D. Kennedy, *J. Chem. Soc., Dalton Trans.*, 1988, 1467.
49 T. L. Venable, W. C. Hutton, and R. N. Grimes, *J. Am. Chem. Soc.*, 1984, **106**, 29.

50 X. L. R. Fontaine, H. Fowkes, N. N. Greenwood, J. D. Kennedy, and M. Thornton-Pett, *J. Chem. Soc., Dalton Trans.*, 1987, 1431; 2417.

51 X. L. R. Fontaine and J. D. Kennedy, *J. Chem. Soc., Chem. Commun.*, 1986, 779.

52 J. D. Kennedy and J. Staves, *Z. Naturforsch., Teil B*, 1979, **34**, 808.

53 W. McFarlane, *Proc. R. Soc. London, Ser. A*, 1986, **306**, 185.

Received 6*th October* 1988; *Paper* 8/03995J